

# Sialons for Ultraprecision Equipment

Shuji Asada\*1  
Masanori Ueki\*1

Toshio Mukai\*1

## Abstract:

*Advanced ceramics are slowly and steadily finding increasing uses as structural materials with the improvement of mechanical properties and the progress of shape imparting technology. The expansion of semiconductor markets and the microfabrication tendency of semiconductor manufacturing processes in recent years have placed ever increasing demands on the accuracy of materials used in equipment for manufacturing and fabricating semiconductors. Against this background, Nippon Steel focused on the future potential of ceramics and sialons in particular and has long worked on the development of sialon manufacturing technology and of sialon products as materials for ultraprecision equipment. This article describes the shapes to which Nippon Steel can produce sialons and the characteristics of sialon products, introduces joining as one elementary technology required for commercialization of sialons, and discusses the rolling contact wear resistance of sialons as an example of characterization.*

## 1. Introduction

Generally, advanced ceramics are said to have heat resistance, stiffness, hardness, specific gravity, chemical resistance, and other properties superior to those of metals and advanced ceramics do not change with time in these properties in air and vacuum at close to room temperature. The manufacturing processes of advanced ceramics commonly consist of preparing a powdered raw material, forming the powder into a compact of desired shape, and sintering the green compact to a product. Since the beginning of the 1980s when raw material powders with uniform purity and particle size were manufactured and marketed, advanced ceramics have gradually improved in properties and

found uses as structural materials. **Table 1** lists the properties of advanced ceramics presently marketed by Nippon Steel (representative types excerpted from Nippon Steel's catalogs of advanced ceramics).

Sialons are characteristic of the advanced ceramics. They combine high specific stiffness (ratio of Young's modulus to density) with low thermal expansion and thermal conductivity in vicinity of room temperature, as compared with alumina ( $\text{Al}_2\text{O}_3$ ), silicon carbide (SiC), and zirconia ( $\text{ZrO}_2$ ). Optimization of process parameters allows sialons to be manufactured with excellent rolling contact wear resistance and surface quality for specific needs.

Nippon Steel introduced the material patents of sialons from Lucas Cookson Syalon (currently Cookson Syalons Ltd.) of England in 1985 and has since carried out the marketing, mer-

\*1 Technical Development Bureau

Table 1 Properties of advanced ceramics marketed by Nippon Steel

Material Material No.	S110	Sialon S120	S140	Alumina A112	Silicon carbide C101	Zirconia Z100	Reference Stainless steel SUS 304
Color	Light gray	Dark gray	Dark gray	White	Black	Milk white	-
Bulk density g/cm <sup>3</sup>	3.24	3.22	3.20	3.95	3.15	6.00	8.03
Young's modulus GPa	290	280	280	380	380	210	200
Hardness Hv	14.5	12.7	12.7	15.2	21.6	12.3	-
Bending strength (RT) MPa	880	690	490	440	490	980	(Tensile strength) 520
Fracture toughness MPa·m <sup>1/2</sup>	6.5	6.0	4.6	3.9	-	3.6	-
Coefficient of thermal expansion ×10 <sup>-6</sup> /°C							
RT-100°C	1.6	1.6	1.5	5.7	2.6	-	-
RT-500°C	2.6	2.5	-	7.1	-	7.8	18.4
Thermal conductivity (RT) W/m°C	21	21	21	23	55	2.7	15

chandising, and manufacturing technology development of sialons as structural ceramics.

This article gives a brief overview of sialons and their manufacturing process, and describes the shapes to which sialons can be manufactured at Nippon Steel, and the properties of sialon products. Joining is discussed as one elementary technology required for commercialization of sialons, and the rolling contact wear resistance of sialons is presented as an example of their characterization.

2. Sialon

Beta-sialon (hereinafter referred to simply as sialon) is such a material that aluminum and oxygen are substitutionally dissolved at the atomic positions of silicon and nitrogen in silicon nitride ( $\beta$ -Si<sub>3</sub>N<sub>4</sub>), respectively, and is expressed by

$$Si_{6-2z}Al_zO_zN_{8-2z} \quad \text{where } 0 < z \leq 4.2 \quad \dots\dots(1)$$

Fig. 1 illustrates the region of the sialon phase in the phase diagram of the Si<sub>3</sub>N<sub>4</sub>-Al<sub>2</sub>O<sub>3</sub>-AlN-SiO<sub>2</sub> pseudoquaternary system at 1,700°C<sup>1)</sup>.

The properties of sialon depend on the properties and composition of raw materials and on such process parameters as forming methods, sintering conditions, and machining methods. Before the actual manufacture of sialon, it is necessary to find out the optimum manufacturing conditions to suit the application and property requirements of sialon parts while considering the manufacturing cost. A general ceramic manufacturing process flow chart is given in Fig. 2.

In the manufacture of sialon, Al<sub>2</sub>O<sub>3</sub> powder, AlN powder, rare-earth oxides like yttrium oxide (Y<sub>2</sub>O<sub>3</sub>) (as sintering aids), organic binders, and solvents are added to Si<sub>3</sub>N<sub>4</sub> powder and processed wet. The particle size of the raw materials ranges from submicrons to a few microns. The wet-processed powder mixture may be formed into a desired shape by a wet or dry method. In the former case, the mixed powder is spray dried into agglomerates, ranging from 50 to a few hundred micrometers in diameter, formed by uniaxial pressing or cold isostatic pressing (CIP). If necessary it is green machined into a compact of the desired shape. In the latter, the wet-processed mixture is poured into a mold and solidified in the mold by slip casting or injection molding. The compact thus obtained has the binder removed in the dewaxing step and is densified in the sintering step. The sintering temperature of sialon varies with the starting materials and mix composition and is generally 1,600 to 1,800°C. The compact is sometimes pressure sintered by hot pressing or hot isostatic pressing (HIP).

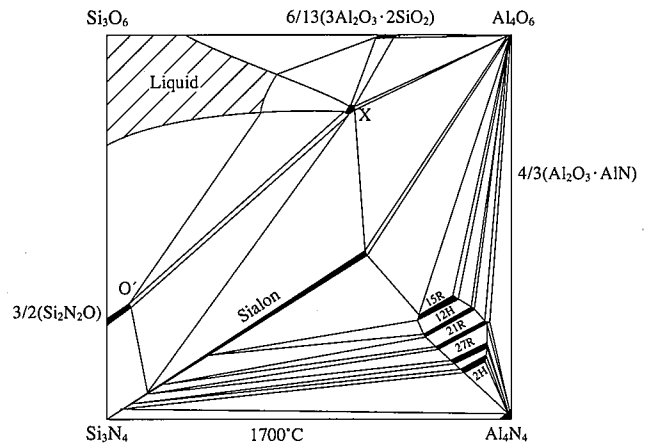


Fig. 1 Phase diagram of Si<sub>3</sub>N<sub>4</sub>-Al<sub>2</sub>O<sub>3</sub>-AlN-SiO<sub>2</sub> system

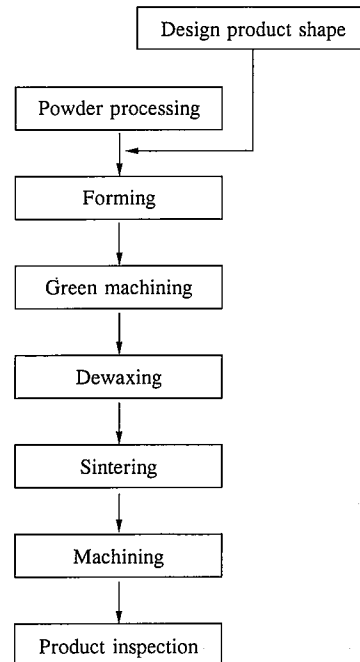


Fig. 2 Flow chart of ceramic product manufacture

The sintering mechanism of sialon is of the dissolution and reprecipitation type as explained below.  $Al_2O_3$  and rare-earth oxides in the raw materials react with  $SiO_2$  on the surfaces of silicon nitride particles to form a liquid phase. Silicon nitride first dissolves in the liquid phase and later precipitates out of the liquid phase as sialon grains. The liquid phase remains as a glassy phase at the grain boundaries. Where heat resistance is required, the glassy phase is generally crystallized. The sintered compact is machined as required. Since sialon is hard and difficult to machine, it is mostly ground with diamond tools. Since not only expensive diamond abrasive grains are consumed, but also the machining rate is slow, sialon costs much more to machine than ordinary metals. Particularly when the compact is large and complex shaped, it must be machined by taking into account sintering shrinkage, deformation, and warpage, among other factors. To minimize the required amount of machining, it is also necessary to produce a desired shape by joining component parts.

### 3. Shapes and Characteristics of Sialon Products

Nippon Steel can manufacture sintered sialon products of any desired shape, measuring 400 by 800 mm or more. **Photo 1** shows an example of a box-shaped sialon part with a minimum wall thickness of 3 to 5 mm. Hollow structural bodies can also be made by utilizing the technology of joining by local sintering<sup>2,3)</sup>.

Applying the technology of machining sintered compacts to very close tolerances, Nippon Steel can produce sialon parts with shape accuracy, surface roughness, and rolling contact wear fatigue resistance<sup>4)</sup> as summarized in **Table 2**.

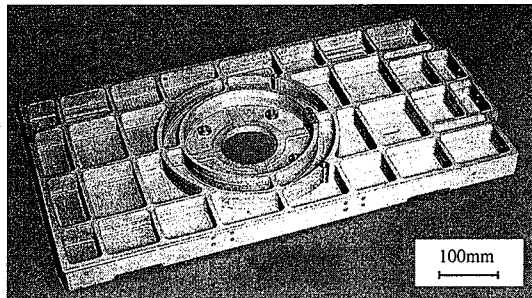


**Photo 1** Large sialon part (model)

**Table 2** Properties of Nippon Steel sialon parts

Straightness, flatness, and parallelism $2 \mu m$	These properties can be attained by development of technology for machining sintered compacts to very close tolerances. Perpendicularity and other geometrical accuracies are as given at left.
Surface roughness $Ra \leq 0.05 \mu m$	Surface roughness depends on material microstructure and machining process. Surface roughness requirement given at left is accomplished by optimization of process conditions. (Example of surface roughness measurement is shown in Fig. 3.)
Rolling contact wear (fatigue) Equal or superior to bearing steel (SUI-2)	Rolling contact wear resistance not inferior to that of bearing steel can be obtained by optimizing process conditions. (Refer to 4.2 in text.)

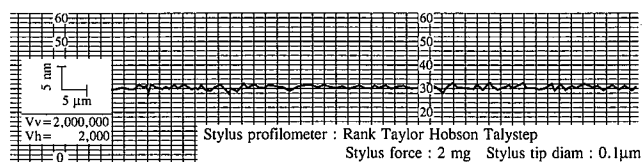


**Fig. 3** Example of surface roughness measurement of Nippon Steel sialon material

Attempts are being made to use sialon as material of construction for precision equipment parts by combining the technology of manufacturing precise, large and complex-shaped parts with high specific stiffness, low coefficient of thermal expansion, and other excellent properties of sialon previously noted. The technology of joining sialon by local sintering<sup>2,3)</sup> and the results of evaluation of rolling contact wear resistance of sialon are described below as one example of technology development to meet these applications.

### 4. Examples of Elementary Technology Development

#### 4.1 Joining of sialon by local sintering

##### 4.1.1 Background and purpose

Various studies have been conducted about the joining of sialon to metal and sialon to sialon. Brazing with active filler metals is widely exploited for joining sialon parts in industry. Especially when manufacturing large complex-shaped parts with sialon alone, sialon parts joined by conventional methods had such problems as lack of specific stiffness and residual stress. These problems called for the development of such joining processes that joined sialon parts can be regarded as single sintered sialon parts.

As noted previously, sintered sialon parts generally consist of sialon grains, measuring a few micrometers or less in size, and glassy phase at the grain boundaries. The authors focused on this grain-boundary glassy phase. Based on the condition that the glassy phase and sialon grains should wet well each other, an adhesive was prepared by mixing a glassy phase forming component (oxide) that would assume a composition approximately equal to that of the grain-boundary glassy phase after joining and the  $Si_3N_4$  powder that is the main ingredient of sialon. The adhesive was used to join sialon parts.

##### 4.1.2 Joining technology

**Fig. 4** shows the region of a Y-Si-Al-O-N glass on the phase diagram of a pseudosexinary system or the  $Si_3N_4-Al_2O_3-AlN-SiO_2$  system to which is added  $Y_2O_3$  and YN. The experimental study set the value of  $z$  in Eq. (1) at 0.2 to define the composition of sialon after sintering and prepared the adhesive so that the ratio of the sialon phase forming components to the adhesive ranged from 50:50 to 80:20. Each type of adhesive was prepared by mixing the specified proportions of  $Al_2O_3$ ,  $SiO_2$ ,  $Y_2O_3$ , and  $Si_3N_4$  powders. Typical adhesive compositions are listed in **Table 3**.

The parts to be joined were  $25 \times 20 \times 5$  mm sialon plates with  $z = 0.2$ , and the faying surfaces were finished to  $R_{max} \leq 6 \mu m$ . The adhesive was wet mixed in ethanol to form a slurry by using a ball mill and applied to the faying surface of one sialon plate at an equivalent solid rate of  $5 \text{ mg/cm}^2$ . The other sialon plate was attached to the coated surface. The two sialon plates were clamped with graphite jigs under a pressure of 2 MPa and heat treated in a nitrogen atmosphere of 1 atm at  $1,600^\circ C$  for 10 min. The braze-

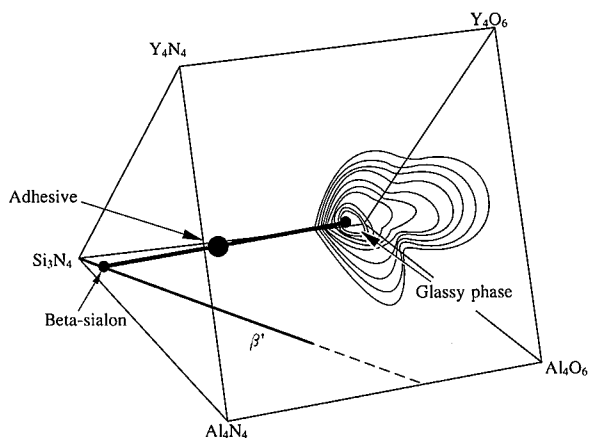


Fig. 4 Adhesive composition region in phase diagram of pseudosequinary system

Table 3 Compositions of sialon adhesives

% $\beta$ -sialon	Adhesive composition (wt%)			
	Si <sub>3</sub> N <sub>4</sub>	Al <sub>2</sub> O <sub>3</sub>	Y <sub>2</sub> O <sub>3</sub>	SiO <sub>2</sub>
20	18.5	8.0	57.0	16.5
30	24.0	9.1	52.1	14.8
50	37.1	10.9	42.0	10.0
60	44.6	12.0	35.9	7.5

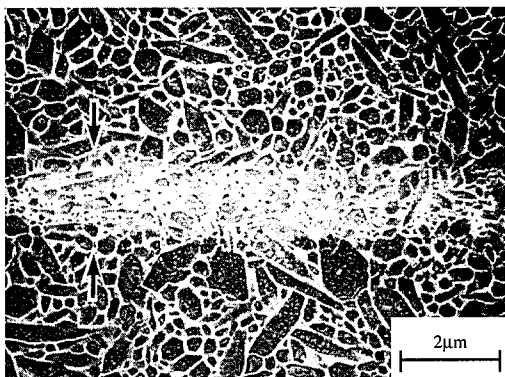


Photo 2 SEM image of joint interface (between arrows)

ment was then tested for bending strength and observed for interfacial microstructure.

#### 4.1.3 Evaluation and application of brazements

Photo 2 shows the scanning electron micrograph of a brazement cross section treated by the plasma etching method. The joint interface is marked by the arrows. The joint is free from voids and inclusions, and a fine-grained sialon microstructure is continuously observed through the lower sialon, interface, and upper sialon. Fig. 5 shows the effect of the composition of the adhesive on the bending strength of brazed joints as determined by four-point bending test with the joint at the center of each specimen. The adhesive composition with a sialon phase/glassy phase ratio of

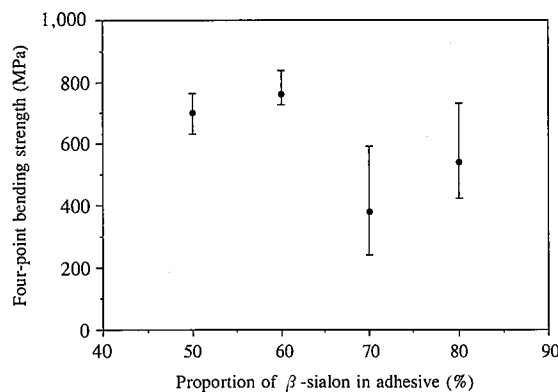


Fig. 5 Effect of sialon phase content of adhesive on four-point bending strength of joints

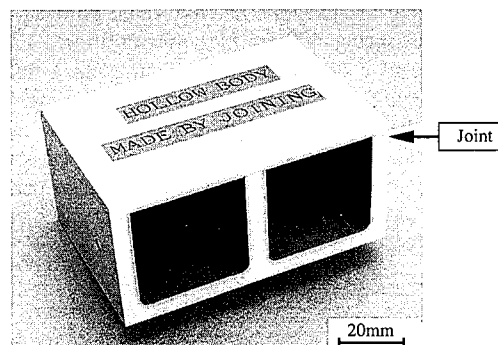


Photo 3 Hollow structural body of sialon made by joining with local sintering (model shape)

60 to 40 provided the highest bending strength, a value comparable to that of parent sialon bodies without joints.

Photo 3 shows an example of hollow sialon structural part fabricated by the proposed joining method. Upper plate was brazed to the hollow box with internally ribbed at certain intervals by the new method. The structure combines light weight with high stiffness.

## 4.2 Rolling contact wear of sialon

### 4.2.1 Background and purpose

Ceramic parts with curved surfaces roll in repeated contact with each other under high stress when used as structural parts, in some applications. Damage to such structural ceramic parts becomes a problem in precision equipment. Using a thrust-type rolling contact wear test machine, sialon parts were tested under specified Hertzian stress for use in such rolling contact applications. The life and fracture mode of sialon were compared with those of other ceramics.

### 4.2.2 Rolling contact wear test method

The thrust-type rolling contact wear test rolls three steel balls on a flat ceramic disk as schematically illustrated in Fig. 6. Pressureless sintered sialon (sialon I) and hot isostatically pressed (HIPed) sialon (sialon II) were used as test materials. Pressureless sintered alumina (Al<sub>2</sub>O<sub>3</sub>), partially stabilized zirconia or PSZ (ZrO<sub>2</sub>), and silicon carbide (SiC) were used as control materials. The specimens were machined from sintered compacts, measuring

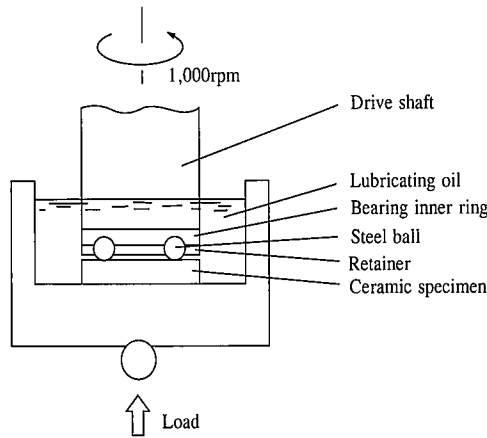


Fig. 6 Schematic illustration of thrust-type rolling contact wear testing machine

about 55×55×10 mm. All materials but SiC (Ibiden SC-850) were home made. Each test surface was rough ground with a #235 diamond wheel, polished to a depth of 50 μm with a #2000 diamond pellet wheel, and polished to a depth of 2 μm with 2 μm or finer abrasives. The surface roughness of the specimens were Ra ≤ 0.05 μm. Each ceramic was loaded to a Hertzian stress of about 5.88 GPa (600 kgf/mm<sup>2</sup>). The steel balls were made from high-chromium bearing steel (JIS G 4805). They were rotated at a speed of 1,000 rpm on the test surface of the specimen under oil lubrication. When the vibration caused by surface damage to the specimen reached a preset value, the specimen was judged to have reached the end of life, and its test was ended.

4.2.3 Rolling contact wear

Fig. 7 shows the Weibull plot of the rolling contact life of the sialons and controls. SiC, Al<sub>2</sub>O<sub>3</sub>, ZrO<sub>2</sub>, pressureless-sintered sialon (sialon I), and HIPed sialon (sialon II) increased in rolling contact wear life in that order.

Photo 4 shows the optical micrographs of the rolling contact surfaces of the controls (a) to (c), pressureless-sintered sialon (d), and HIPed sialon (e). The mode of surface damage varies with the type of ceramic. Arc-shaped cracks, and surface layer spalling and chipping are observed in the controls Al<sub>2</sub>O<sub>3</sub>, ZrO<sub>2</sub>, and SiC. The pressureless-sintered sialon (sialon I) shows no cracks but chipping in some portions of the rolling contact surface. No cracks and

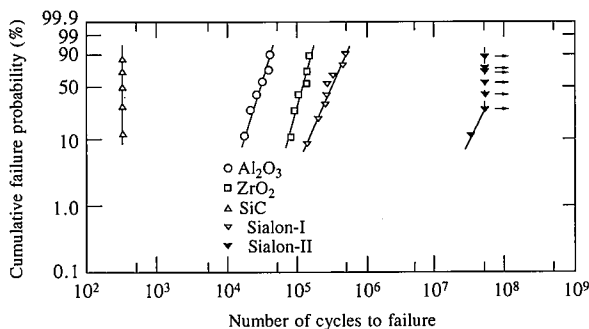


Fig. 7 Rolling contact wear of Nippon Steel ceramics

chipping are observed on the rolling contact surface of the specimen of the HIPed sialon (sialon II) whose test was discontinued after 5×10<sup>7</sup> cycles.

The radius a of a crack that is referred to as the “Hertzian crack” and caused when a hard ball of the radius r is pressed against a flat ceramic disk under the load P is given by

$$a = [3/4\pi r[(1 - \nu_1^2)/E_1 + (1 - \nu_2^2)/E_2]P]^{1/2} \dots\dots(2)$$

where  $\nu_1$  = Poisson’s ratio of the ball;  $E_1$  = Young’s modulus of the ball;  $\nu_2$  = Poisson’s ratio of the disk; and  $E_2$  = Young’s modulus of the disk. The calculated values of a are given in Table 4. As shown on the rolling contact surface photographs in Photo 4, the size of circles with the calculated radius agrees well with that of Hertzian cracks observed on each ceramic.

The tensile stress produced by Hertzian contact in the disk surface is cited as one cause for the occurrence of the Hertzian crack. The maximum tensile stress  $\sigma_{max}$  is produced at the edge of the contact surface and calculated by

$$\sigma_{max} = (1 - 2\nu)Q/3 = (1 - 2\nu)P/2\pi a^2 \dots\dots(3)$$

where  $\nu$  = Poisson’s ratio; Q = maximum Hertzian stress (= 3P/2πa<sup>2</sup>); P = load; and a = radius of the Hertzian crack (Hertzian contact region) described above.

The values of  $\sigma_{max}$  calculated by Eq. (3) for the ceramics are shown in Table 4. The Hertzian cracks are produced when the

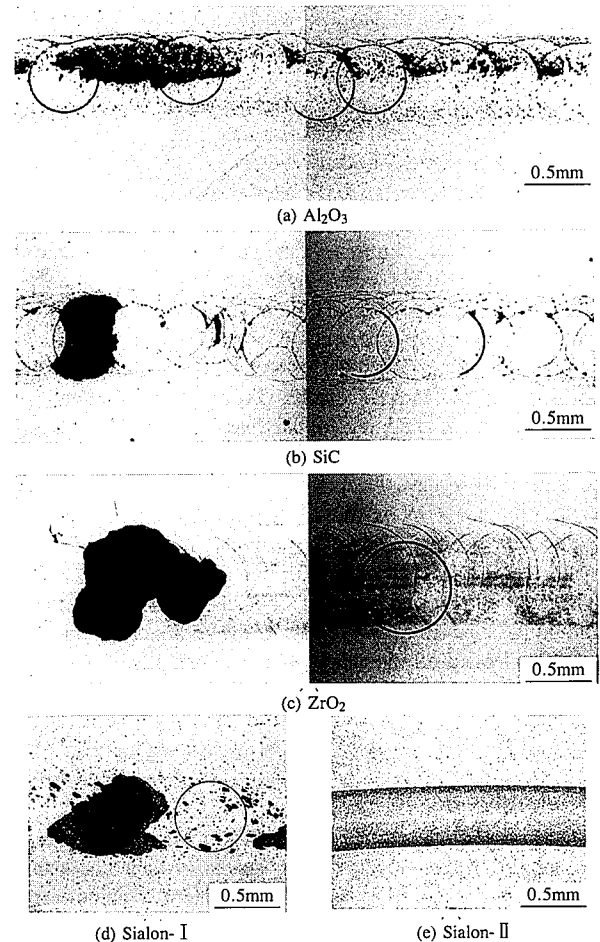


Photo 4 Damage to rolling contact surfaces of ceramics

Table 4 Hertzian stress and three-point bending strength of ceramics

Material [Sintering method]	Alumina Al <sub>2</sub> O <sub>3</sub> [PLS] <sup>1)</sup>	Zirconia ZrO <sub>2</sub> [PLS]	Silicon carbide SiC [PLS]	Sialon	
				I [PLS]	II [PLS+HIP <sup>2)</sup> ]
Load P×3 (kN)	3.26	5.33	3.35	3.92	3.92
Hertzian stress Q (MPa)	5,880	5,879	5,880	5,859	5,877
Radius of Hertzian contact area a (mm)	0.297	0.380	0.301	0.326	0.326
Maximum tensile stress caused by Hertzian contact σ <sub>max</sub> (MPa)	866	725	1,337	871	865
Three-point bending strength of specimen σ <sub>3PB</sub> (MPa)	607	1,176	570	882	1,176
Hertzian crack	○	○ <sup>3)</sup>	○	×	×

<sup>1)</sup> PLS : pressureless sintering, <sup>2)</sup> HIP : hot isostatic pressing, <sup>3)</sup> Hertzian crack is produced after loss of strength by phase transformation.

maximum tensile stress  $\sigma_{\max}$  is greater than the tensile strength of the material concerned. Assuming as first approximation that the three-point bending strength  $\sigma_{3PB}$  is practically equal to the tensile strength of the material, the calculated value of  $\sigma_{\max}$  can be compared with the three-point bending strength of the material to judge whether or not Hertzian cracks will occur in the material. This criterion is given by Eq. (4).

$$\sigma_{\max} \geq \sigma_{3PB} \quad \dots\dots(4)$$

The optical micrographs of **Photo 4** show that Eq. (4) holds true except for ZrO<sub>2</sub>. No cracks are observed in ZrO<sub>2</sub> specimens whose test was discontinued in the early stage, or after  $1.2 \times 10^4$  cycles or about 10% of the average life. It is clear that cracks occurred after a certain number of rolling contact cycles. This suggests that the phase transition induced by the stress (and strain consequently stored) applied by rolling contact to the specimen caused the loss of strength near the surface of the specimen and produced Hertzian cracks in that region.

The wear depth varies from material to material. The rolling contact track groove was relatively shallow and formed wide along Hertzian cracks for alumina. The surface portions near the Hertzian cracks brittlely failed, with the failure initiated at the Hertzian cracks. SiC revealed Hertzian cracks of some depth and had surface spalls at the intersections of the Hertzian cracks.

Unlike Al<sub>2</sub>O<sub>3</sub> and SiC, the pressureless-sintered and HIPed sialons showed no Hertzian cracks. Their life was longer by at least two orders of magnitude than that of the other ceramics. Given the fact that the life of the sialon HIPed to eliminate pores is more than  $10^7$  cycles, the pressureless-sintered sialon probably chipped from pores in or directly below the surface. It is discussed also for bearing steels that sources of failure in rolling contact test lie in the surface and subsurface regions<sup>9)</sup>.

The above-mentioned rolling contact fatigue characteristics depend on the mechanical properties of the ceramics and are hence expected to depend on the shape, size and manufacturing process of sintered compacts. It is confirmed that specimens machined from sintered compacts of about 400×800 mm show rolling contact fatigue strength comparable to that of sintered compacts.

## 5. Conclusions

The technology developed to manufacture sialon ceramic parts for ultraprecision equipment and the results of their characterization have been introduced as part of Nippon Steel's sialon research and development efforts. We will continue our efforts to find more uses for sialon products in the ultraprecision equipment field.

## References

- 1) Thompson, D.P. et al.: Ceramic Materials and Components for Engines. Proceedings of the Second International Symposium. 1986, p. 643-650
- 2) Walls, P.A., Ueki, M.: J. Am. Ceram. Soc. 75 (9), 2491-2497 (1992)
- 3) Walls, P.A., Ueki, M.: J. Am. Ceram. Soc. 78 (4), 999-1005 (1995)
- 4) Asada, S., Fukuda, K., Ueki, M.: J. Ceram. Soc. Japan. 105, 238-240 (1997)
- 5) Littmann, W.E., Winder, R.L.: Trans. of ASME. J. of Basic Engineering. (1966, Sept.), 624